Polydispersity effects on the magnetization of diluted ferrofluids: a lognormal analysis*

Wang Xu-Fei(王旭飞)[a)b)†] and Shi Li-Qun(施立群)[a)b)]

[a)] *Applied Ion Beam Physics Laboratory, Fudan University, Key Laboratory of the Ministry of Education, Shanghai* 200433, *China*
[b)] *Institute of Modern Physics, Department of Nuclear Science and Technology, Fudan University, Shanghai* 200433, *China*

(Received 3 January 2010; revised manuscript received 15 April 2010)

Based on a lognormal particle size distribution, this paper makes a model analysis on the polydispersity effects on the magnetization behaviour of diluted ferrofluids. Using a modified Langevin relationship for the lognormal dispersion, it first performs reduced calculations without material parameters. From the results, it is extrapolated that for the ferrofluid of lognormal polydispersion, in comparison with the corresponding monodispersion, the saturation magnetization is enhanced higher by the particle size distribution. It also indicates that in an equivalent magnetic field, the lognormally polydispersed ferrofluid is magnetically saturated faster than the corresponding monodispersion. Along the theoretical extrapolations, the polydispersity effects are evaluated for a typical ferrofluid of magnetite, with a dispersity of $\sigma = 0.20$. The results indicate that the lognormal polydispersity leads to a slight increase of the saturation magnetization, but a noticeable increase of the speed to reach the saturation value in an equivalent magnetic field.

Keywords: ferrofluid, polydispersity effects, lognormal distribution

PACC: 7550M, 7560J

1. Introduction

A ferrofluid is composed of small (3–15 nm) solid, ferromagnetic, and single-domain particles coated with a molecular layer of dispersant and suspended in a liquid carrier.[1] Showing a normal liquid behaviour coupled with superparamagnetic properties, ferrofluids have been widely used in engineering such as sealing, lubricant, and density separation. In recent years, the medical researches of hyperthermia cancer therapy[2] and magnetic resonance imaging[3] are also using ferrofluids as candidate materials. In a ferrofluid of diluted and monodispersed nanoparticles, the inter-particle interaction is negligible[4,5] and the superparamagnetism is typically described by the Langevin equation.[6−8] However, real ferrofluids are often composed of polydispersed nanoparticles,[9−12] and strictly, the polydispersity may have an additional influence on the magnetization behaviour of the ferrofluids. In this work, a model analysis is made on the polydispersity effects by using a lognormal distribution model of the particle size. To avoid the computing difficulty of nanomaterial parameters, reduced calculations are first performed, and then extrapolated to a real example of magnetite ferrofluids.

2. Lognormal model analysis

For the ferrofluids of monodispersed nanoparticles in a low concentration (e.g., the solid volume fraction $\psi < 0.01$), the inter-particle interaction can be neglected and the collective magnetization is usually described by the Langevin equation[6−8] as

$$M_{\rm m} = M_{\rm ms}\left(\coth\xi - \frac{1}{\xi}\right) = \psi M_{\rm d}\left(\coth\xi - \frac{1}{\xi}\right) = nM_{\rm d}V_{\rm m}L(\xi), \quad \left(\xi = \frac{\mu_0 M_{\rm d} V_{\rm m} H}{kT}\right), \tag{1}$$

where $M_{\rm d}$ is the domain magnetization, $V_{\rm m}$ the solid volume and n the number density of the ferromagnetic nanoparticles, H is magnetic field intensity, $\psi = nV_{\rm m}$ is the solid volume fraction, $M_{\rm m}$ is the collective magnetization and $M_{\rm ms} = nM_{\rm d}V_{\rm m}$ the saturation magnetization of the ferrofluids, μ_0 is the permeability of free space, $k = 1.38 \times 10^{-23}$ is Boltzmann constant and T is absolute temperature.

However, real ferrofluids are usually composed of polydispersed nanoparticles, whose polydispersity is typically described by a lognormal distribution model,[9−12] as given by

$$p(r) = \frac{1}{\sqrt{2\pi}\sigma r}\exp\left[\frac{-(\ln r - \ln R)^2}{2\sigma^2}\right]$$

*Project supported by the Shanghai Leading Academic Discipline Project of China (Grant No. B107).
†Corresponding author. E-mail: xufei.wang@gmail.com
© 2010 Chinese Physical Society and IOP Publishing Ltd

$$= \frac{1}{\sqrt{2\pi}\sigma r}\exp\left[\frac{-\left(\ln\left(r/R\right)\right)^2}{2\sigma^2}\right], \quad (2)$$

where r is the particle radius, $\ln R$ is the mean value and σ is the standard deviation of $\ln r$. From Eq. (2), the mean value E and standard deviation Sd of the particle radius are derived as

$$E = \exp\left(\ln\left(R\right) + \sigma^2/2\right),$$
$$Sd = \exp\left(\ln\left(R\right) + \sigma^2/2\right)\cdot\sqrt{\exp\left(\sigma^2\right) - 1}. \quad (3)$$

Conversely, R and σ can be expressed by E and Sd as

$$R\left(E, Sd\right) = \exp\left[\ln\left(E\right) - \frac{1}{2}\ln\left(1 + \left(\frac{Sd}{E}\right)^2\right)\right],$$
$$\sigma\left(E, Sd\right) = \sqrt{\ln\left(1 + \left(\frac{Sd}{E}\right)^2\right)}. \quad (4)$$

According to the lognormal model, the solid volume fraction of the particles is

$$\psi = \int_0^\infty \frac{4\pi r^3}{3} np(r)\mathrm{d}r, \quad (5)$$

and the collective magnetization M_p of the polydispersed ferrofluid is

$$M_p = \int_0^\infty \frac{4\pi r^3 M_\mathrm{d}}{3} np(r)\left(\int_0^\pi \cos\theta q(\theta)\mathrm{d}\theta\right)\mathrm{d}r, \quad (6)$$

where θ is the angle between the magnetic moment of the particles and the magnetic field, and

$$q(\theta)\mathrm{d}\theta = \frac{\exp\left(\alpha\cos\theta\right)\sin\theta\mathrm{d}\theta}{\int_0^\pi \exp\left(\alpha\cos\theta\right)\sin\theta\mathrm{d}\theta},$$
$$\alpha = \frac{\mu_0 M_\mathrm{d} V_\mathrm{m} H}{kT} = \frac{4\pi r^3 \mu_0 M_\mathrm{d} H}{3kT}, \quad (7)$$

thus

$$M_\mathrm{p} = \int_0^\infty \frac{4\pi r^3 M_\mathrm{d}}{3} np(r) \times \left(\int_0^\pi \frac{\exp\left(\alpha\cos\theta\right)\cos\theta\sin\theta\mathrm{d}\theta}{\int_0^\pi \exp\left(\alpha\cos\theta\right)\sin\theta\mathrm{d}\theta}\right)\mathrm{d}r. \quad (8)$$

Let x denote $\cos\theta$, the magnetization of the lognormal polydispersion is derived as

$$M_\mathrm{p} = \int_0^\infty \frac{4\pi r^3 M_\mathrm{d}}{3} np(r)\left(\frac{\int_{-1}^1 \exp\left(\alpha x\right) x\mathrm{d}x}{\int_{-1}^1 \exp\left(\alpha x\right)\mathrm{d}x}\right)\mathrm{d}r = M_\mathrm{d}\int_0^\infty \frac{4\pi r^3}{3} np(r)\left(\coth\left(\alpha\right) - \frac{1}{\alpha}\right)\mathrm{d}r$$
$$= M_\mathrm{d}\int_0^\infty \psi(r)\cdot L\left[\alpha\left(r\right)\right]\mathrm{d}r, \quad \left(\psi(r) = \frac{4\pi r^3}{3} np(r), \quad \alpha(r) = \frac{4\pi r^3 \mu_0 M_\mathrm{d} H}{3kT}\right), \quad (9)$$

and the saturation magnetization M_ps is given by

$$M_\mathrm{ps} = M_\mathrm{d}\int_0^\infty \frac{4\pi r^3}{3} np(r)\mathrm{d}r = M_\mathrm{d}\int_0^\infty \psi(r)\mathrm{d}r. \quad (10)$$

To avoid the computing difficulty on the nanomaterial parameters n and M_d, the polydispersity effects can be evaluated in reduced expressions as follows:

$$M_\mathrm{ms} = nM_\mathrm{d}\frac{4\pi E^3}{3} \rightarrow \psi_\mathrm{ms} = E^3, \quad (11)$$

$$M_\mathrm{ps} = M_\mathrm{d}\int_0^\infty \frac{4\pi r^3}{3} np(r)\mathrm{d}r \rightarrow \psi_\mathrm{ps} = \int_0^\infty \frac{r^2}{\sqrt{2\pi}\sigma(E, Sd)}\exp\left[-\frac{1}{2}\left(\frac{\ln\left(r/R(E, Sd)\right)}{\sigma(E, Sd)}\right)^2\right]\mathrm{d}r, \quad (12)$$

where E is the mean value and Sd is the standard deviation of the variable r.

According to Eqs. (11) and (12), the dependence of ψ_ps on E for different Sd is calculated in a convenient range, as shown in Fig. 1(a). It can be seen that due to the polydispersity, the function value of $\psi_\mathrm{ps}(E)$ is enhanced higher than the corresponding $\psi_\mathrm{ms}(E)$ on equivalent E. Moreover, for a constant Sd, the logarithm of ψ_ps displays a V-shape curve on E, i.e., when E decreases but still higher than a critical value, $\psi_\mathrm{ps}(E)$ decreases with E, showing a positive dependence; when E is below the critical value, the curve of $\psi_\mathrm{ps}(E)$ turns back and increases to positive infinity with the decreasing E, showing a negative dependence. The critical value is analytically determined as $E_0 = Sd$. Mathematically, the V-shape curve behaviour of $\psi_\mathrm{ps}(E)$ is due to the influence of $p(r)$ on the integral value of $\int_0^\infty r^3 p(r)\mathrm{d}r$.

For a clearer illustration, the binary dependence of $\psi_\mathrm{ps}(E,\ Sd)$ is plotted in Fig. 1(b), with three typical curves highlighted, i.e., the curve of $Sd = 0$ for monodispersion, of a typical dispersity $\sigma = 0.2$ for

common ferrofluids,[13] and of $Sd = E$ as the critical line between the positive and negative parts of the $\psi_{\rm ps}(E)$ curves. It can be seen that for a constant E, $\psi_{\rm ps}$ is positively dependent on Sd, and from the curve of $\sigma = 0.2$, one can see that the typical dispersity leads to a slight increase of $\psi_{\rm ps}$, in comparison with the corresponding value of $\psi_{\rm ms}$.

To evaluate the difference between $\psi_{\rm ps}$ and $\psi_{\rm ms}$, the curve of $\psi_{\rm ps}/\psi_{\rm ms}$ on E is plotted in Fig. 1(c) and 1(d) in convenient ranges. It can be seen that for a constant Sd, the value of $\psi_{\rm ps}/\psi_{\rm ms}$ is negatively dependent on E; whereas for a constant E, the value is positively dependent on Sd.

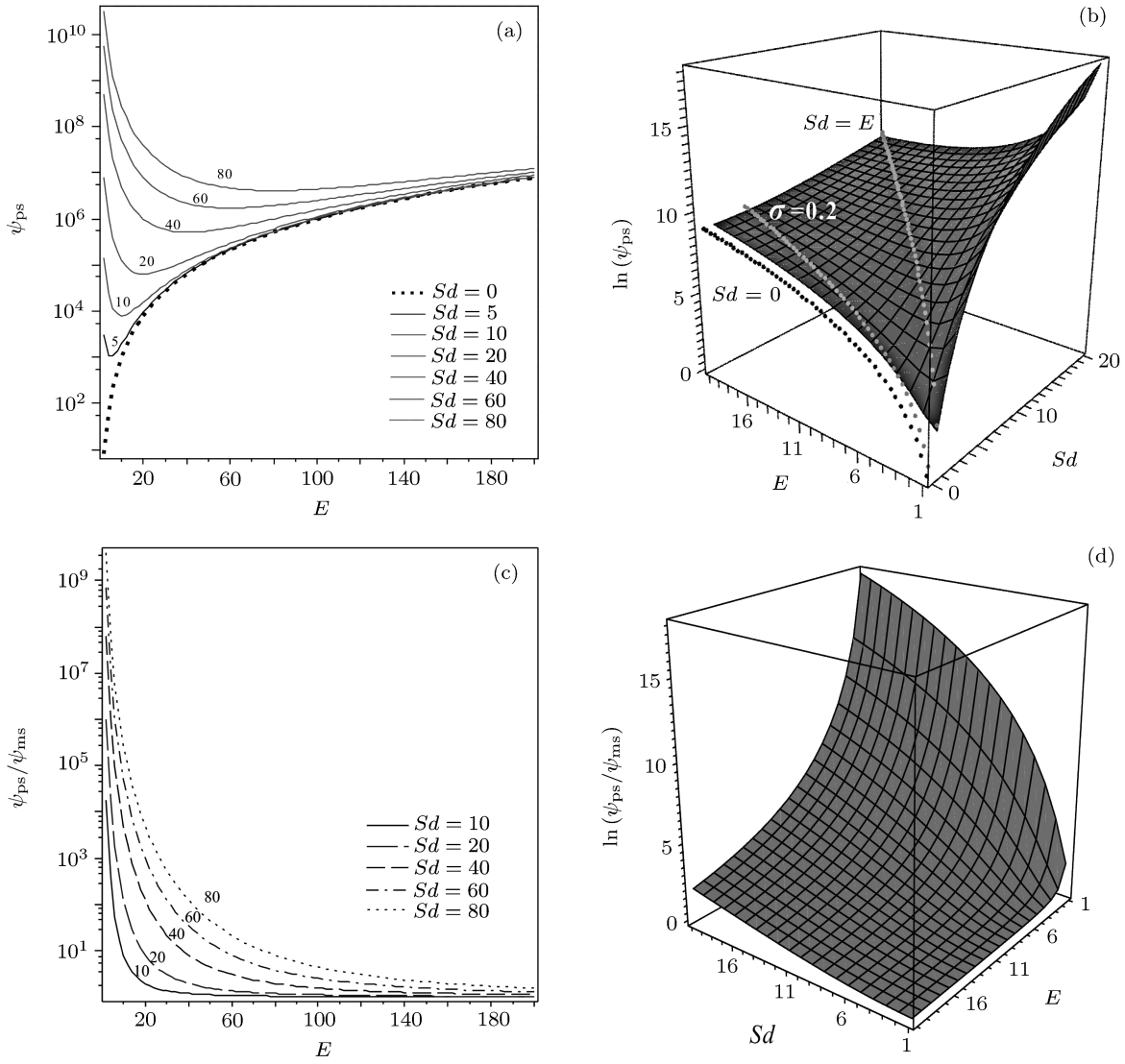


Fig. 1. (a) The dependence of $\psi_{\rm ps}$ on E (logarithmic coordinates), for different values of Sd. (b) The binary dependence of $\ln(\psi_{\rm ps})$ on E and Sd, with the curves of $\sigma = 0.20$, $Sd = 0$ and $Sd = E$ highlighted on the 3D surface. (c) The dependence of $\psi_{\rm ps}/\psi_{\rm ms}$ on E (logarithmic coordinates) for different Sd. (d) The binary dependence of $\ln(\psi_{\rm ps}/\psi_{\rm ms})$ on E and Sd.

To evaluate the polydisperity effects on the magnetization process of the diluted ferrofluids, the equilibrium magnetization curves of $M_{\rm p}$ and the normalized curve of $M_{\rm p}/M_{\rm ps}$ are respectively compared with the corresponding curves of $M_{\rm m}$ and $M_{\rm m}/M_{\rm ms}$ on an equivalent magnetic field. Similarly, the $M_{\rm m}$–H relationship in Eq. (1) is reduced as

$$\psi_{\rm m} = r^3 \left(\coth\left(r^3 H\right) - \frac{1}{r^3 H} \right) = r^3 L(r^3 H), \tag{13}$$

and the $M_{\rm p}$–H relationship in Eq. (9) is reduced as

$$\psi_{\rm p} = \int_0^\infty r^2 \frac{1}{\sqrt{2\pi}\sigma\left(E, Sd\right)} \exp\left[\frac{-\left(\ln\left(r/R\left(E, Sd\right)\right)\right)^2}{2\left(\sigma\left(E, Sd\right)\right)^2}\right]\left(\coth\left(r^3H\right) - \frac{1}{r^3H}\right) {\rm d}r. \tag{14}$$

According to Eqs. (11)–(14), the normalized value of $M_{\rm m}/M_{\rm ms}$ on H is reduced as

$$\frac{\psi_{\rm m}}{\psi_{\rm ms}} = \left(\coth\left(r^3H\right) - \frac{1}{r^3H}\right) = L(r^3H), \tag{15}$$

and the relationship of $M_{\rm p}/M_{\rm ps}$ on H is reduced as

$$\frac{\psi_{\rm p}}{\psi_{\rm ps}} = \frac{\int_0^\infty r^2 \frac{1}{\sqrt{2\pi}\sigma\left(E, Sd\right)} \exp\left[\frac{-\left(\ln\left(r/R\left(E, Sd\right)\right)\right)^2}{2\left(\sigma\left(E, Sd\right)\right)^2}\right]\left(\coth\left(r^3H\right) - \frac{1}{r^3H}\right) {\rm d}r}{\int_0^\infty r^2 \frac{1}{\sqrt{2\pi}\sigma\left(E, Sd\right)} \exp\left[\frac{-\left(\ln\left(r/R\left(E, Sd\right)\right)\right)^2}{2\left(\sigma\left(E, Sd\right)\right)^2}\right] {\rm d}r}. \tag{16}$$

According to Eqs. (13)–(16), the curves of $\psi_{\rm p}(H)$ and the corresponding $\psi_{\rm m}(H)$ are plotted in Fig. 2(a). The normalized curves of $\psi_{\rm p}/\psi_{\rm ps}(H)$ and $\psi_{\rm m}/\psi_{\rm ms}(H)$ are plotted in Fig. 2(b) for constant E and different Sd, and in Fig. 2(c) for different E and different Sd.

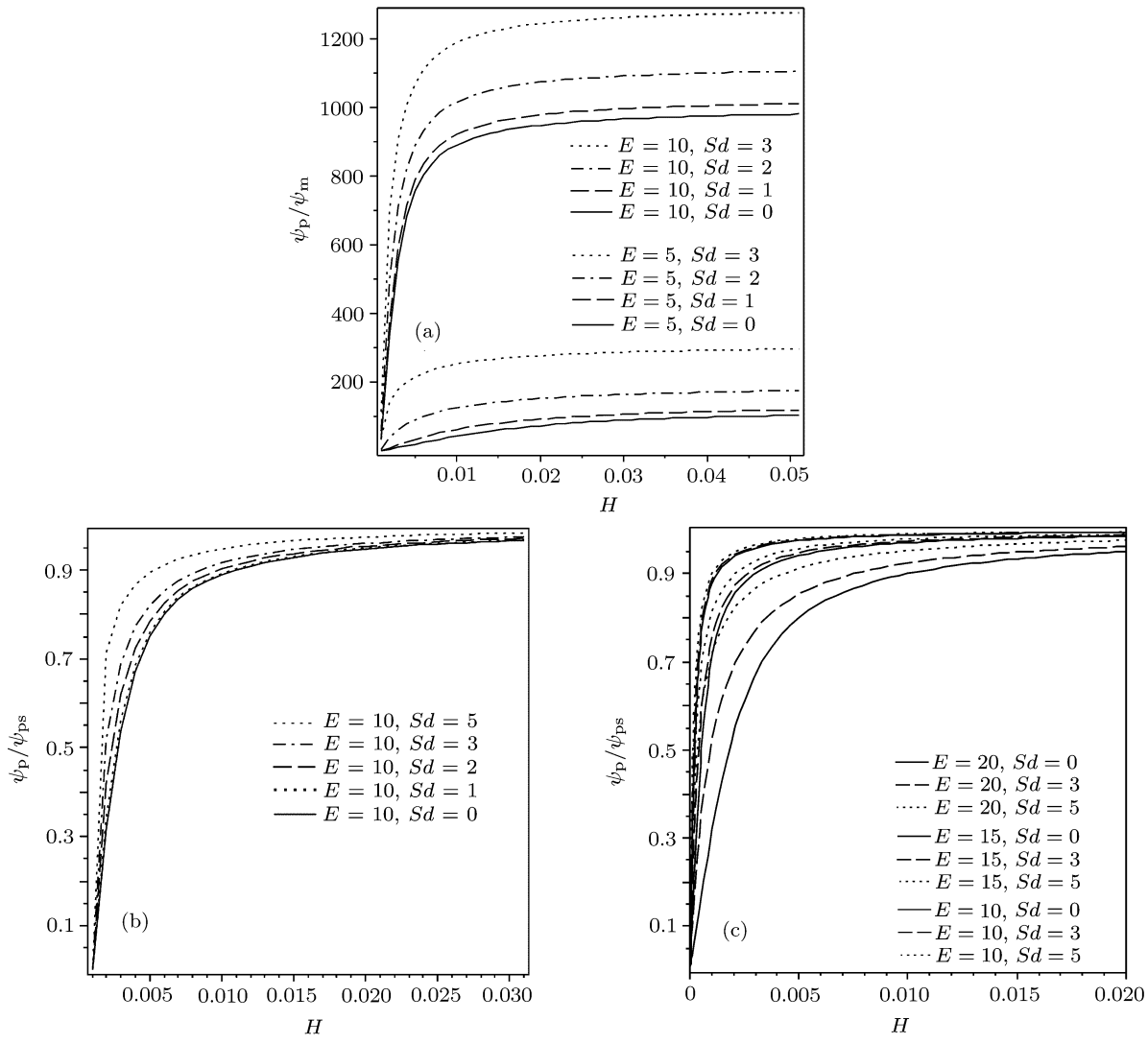


Fig. 2. (a) The curves of $\psi_{\rm p}$ and the corresponding $\psi_{\rm m}$ versus H for different E and Sd. (b) The normalized curves of $\psi_{\rm p}/\psi_{\rm ps}$ versus H for constant E and different Sd, in comparison with the corresponding curve of $\psi_{\rm m}/\psi_{\rm ms}$. (c) The normalized curves of $\psi_{\rm p}/\psi_{\rm ps}$ versus H, with the corresponding curves of $\psi_{\rm m}/\psi_{\rm ms}$, for different values of E and Sd.

All the curves are plotted in convenient ranges of H, with proper values of E and Sd. From Fig. 2(a), one can see that on an equivalent H, the curves of $\psi_{\rm p}(H)$ have the similar shape but higher values in comparison with the Langevin curve of $\psi_{\rm m} = E^3 L(E^3 H)$. In Fig. 2(b), the normalized curves of $\psi_{\rm p}/\psi_{\rm ps}(H)$ are compared with the curve of $\psi_{\rm m}/\psi_{\rm ms}(H)$. One can see that for a constant E, $\psi_{\rm p}/\psi_{\rm ps}(H)$ has higher value than $\psi_{\rm m}/\psi_{\rm ms}(H)$ on equivalent H, and the value of $\psi_{\rm p}/\psi_{\rm ps}(H)$ is positively dependent on Sd. Besides, the curve of $\psi_{\rm p}/\psi_{\rm ps}(H)$ has a faster approach to 1 than the normalized Langevin curve of $\psi_{\rm m}/\psi_{\rm ms} = L(E^3 H)$. Further in Fig. 2(c), one can see that for an equivalent H, the values of $\psi_{\rm m}/\psi_{\rm ms}(H)$ and $\psi_{\rm p}/\psi_{\rm ps}(H)$ are both positively dependent on E, and for a constant Sd and a higher E, the curve of $\psi_{\rm p}/\psi_{\rm ps}(H)$ has a faster approach to 1 with the increasing H.

For further analysis, the difference between $\psi_{\rm p}/\psi_{\rm ps}$ and $\psi_{\rm m}/\psi_{\rm ms}$, as a function of H, is plotted in Fig. 3. It can be seen that for an increasing H, the value of $\psi_{\rm p}/\psi_{\rm ps}$–$\psi_{\rm m}/\psi_{\rm ms}$ increases sharply to maximum values, then slowly decreases to zero. For a constant E, the value of $\psi_{\rm p}/\psi_{\rm ps}$–$\psi_{\rm m}/\psi_{\rm ms}$ is positively dependent on Sd, as shown in Fig. 3(a); whereas for a constant Sd, the value is negatively dependent on E, as shown in Fig. 3(b).

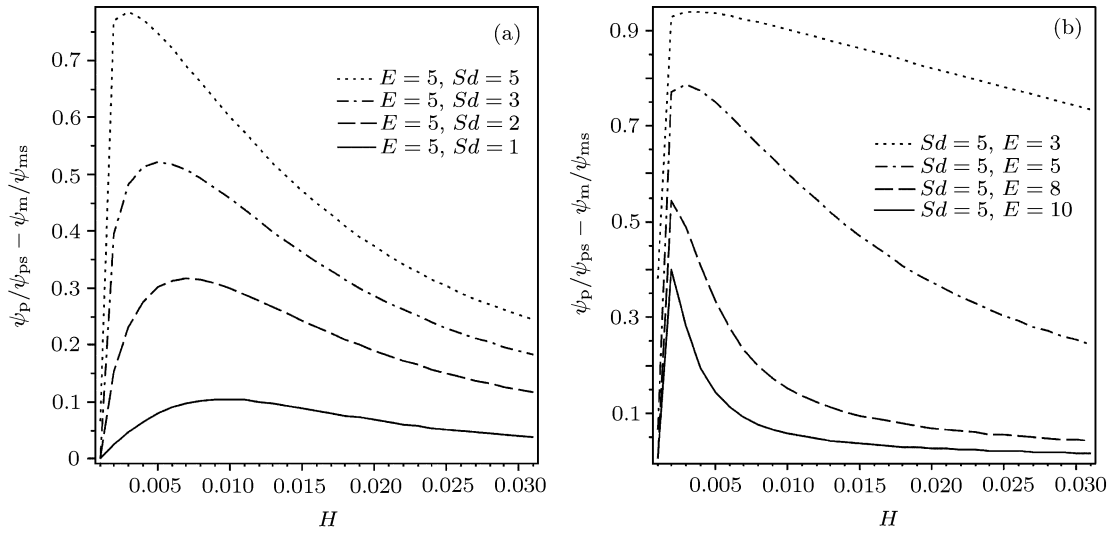


Fig. 3. (a) The dependence curves of ($\psi_{\rm p}/\psi_{\rm ps}$–$\psi_{\rm m}/\psi_{\rm ms}$) versus H, for a constant mean value E ($E = 5$) and different standard deviations (Sd = 1, 2, 3, 5). (b) The dependence curves of ($\psi_{\rm p}/\psi_{\rm ps}$–$\psi_{\rm m}/\psi_{\rm ms}$) versus H, for a constant standard deviation Sd ($Sd = 5$) and different mean values E (E = 3, 5 8, 10).

3. Real ferrofluids

Considering the typical ferrofluids of magnetite nanoparticles, with the domain magnetization $M_{\rm d}$ = 446 kA/m, the anisotropy constant $K_{\rm u} = 32$ kJ·m^{-3}, the particle number density $n = 10^{16}$, the carrier liquid viscosity $\eta = 0.001$ Pa·s, the measurement time $\tau = 100$ s and the ambient temperature $T = 300$ K, for exhibiting an intrinsic superparamagnetism by Néel relaxation, the critical radius of the magnetite nanoparticles is determined as $R_{\rm sp} = 9.2$ nm; for an extrinsic superparamagnetism by Brownian relaxation, the critical radius is $R'_{\rm sp} = 3205$ nm.[14–16] Because the critical radius of single-domain magnetite is about 64 nm,[17] diluted and monodispersed ferrofluids of single-domain magnetite particles usually exhibit a superparamagnetism state. For a lognormal polydispersion, the upper limit of the mean particle radius should be below 64 nm. For example, for the standard deviations Sd = 1, 5 and 10 nm, the integral of $p(r)$ within 0–64 nm on E are plotted in Fig. 4. To ensure a majority (e.g., 99%) of single-domain particles, the upper limits of the mean radii are respectively determined as 61.64 nm, 51.25 nm and 34.2 nm, as indicated by the horizontal dashed line and the arrows.

The saturation magnetization of the magnetite ferrofluids is calculated and the results give $M_{\rm ps}/M_{\rm ms} \approx 1.95$ for $E = 10$ nm, $Sd = 5$ nm, $M_{\rm ps}/M_{\rm ms} \approx 1.29$ for $E = 10$ nm, $Sd = 3$ nm, and $M_{\rm ps}/M_{\rm ms} \approx 1.20$ for $E = 20$ nm, $Sd = 5$ nm, indicating a noticeable increase of saturation magnetization due to the lognormal polydispersity. However, for the typical dispersity (e.g., $\sigma = 0.2$, standard deviation of $\ln r$) of common ferrofluids, when the mean particle sizes are $E = 25$ nm, 20 nm, 15 nm, 10 nm, and 5 nm, the corresponding standard deviations are $Sd = 5$ nm, 4 nm, 3 nm, 2 nm, and 1 nm, and for all the values, $M_{\rm ps}/M_{\rm ms} \approx 1.12$. Therefore, the common dispersity

only leads to a slight increase of saturation magnetization for typical magnetite ferrofluids.

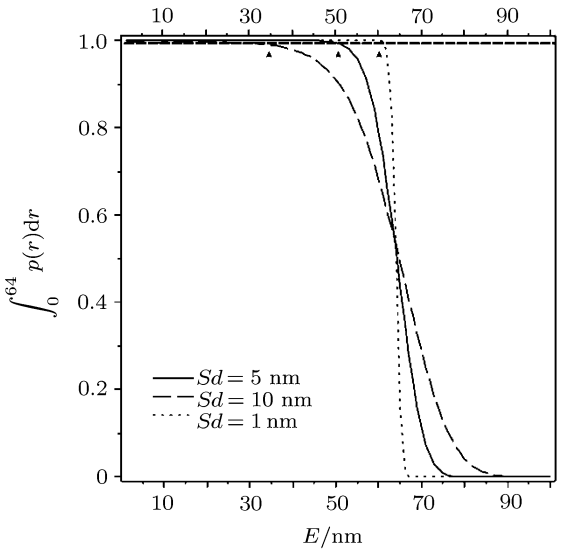


Fig. 4. The dependence of the integral of $p(r)$ within $0 \sim 64$ nm on the mean particle size, for different standard deviations of the particle size.

To evaluate the polydispersity effects on the magnetization processes of the magnetite ferrofluids, the curves of $M_\mathrm{p}/M_\mathrm{ps}$–$M_\mathrm{m}/M_\mathrm{ms}$ on magnetic field H are plotted in Fig. 5, corresponding to the curves of $\psi_\mathrm{p}/\psi_\mathrm{ps}$–$\psi_\mathrm{m}/\psi_\mathrm{ms}$ versus H in Fig. 3. The normalized values $M_\mathrm{p}/M_\mathrm{ps}$ and $M_\mathrm{m}/M_\mathrm{ms}$ represent the degree of saturation magnetization. It can be seen that the difference between $M_\mathrm{p}/M_\mathrm{ps}$ and $M_\mathrm{m}/M_\mathrm{ms}$ is clearly dependent on the mean particle size, but little influenced by the different standard deviations. For each of the mean sizes, the curves of different standard deviations are almost overlapped, i.e., each line in Fig. 5 actually represents four overlapped curves of the different standard deviations. In the calculation ranges of $E < 25$ nm and $Sd < 10$ nm, $M_\mathrm{p}/M_\mathrm{ps}$–$M_\mathrm{m}/M_\mathrm{ms}$ gives a maximum value at around $H = 200$ A·m^{-1}, and the maximum is calculated as 0.75 for $E = 25$ nm, 0.85 for $E = 20$ nm, 0.94 for $E = 15$ nm, 0.98 for $E = 10$ nm and 0.998 for $E = 5$ nm, respectively. For the common dispersity $\sigma = 0.2$, when $E = 25$ nm, 20 nm, 15 nm, 10 nm, and 5 nm, the corresponding standard deviations are $Sd = 5$ nm, 4 nm, 3 nm, 2 nm, and 1 nm, all below 10 nm, thus the curves of $M_\mathrm{p}/M_\mathrm{ps}$–$M_\mathrm{m}/M_\mathrm{ms}$ versus H should be identical with the curves in Fig. 5. These results indicate that in an equivalent increasing magnetic field, the magnetite ferrofluids of lognormal polydispersity have higher magnetization value and faster speed to saturation than the corresponding monodispersion. For the typical dispersity value of common ferrofluids, the maximum difference between $M_\mathrm{p}/M_\mathrm{ps}$ and $M_\mathrm{m}/M_\mathrm{ms}$ appears at a weak field $H = 200$ A·m^{-1}. The difference has a noticeable negative dependence on the mean value, but a negligible influence by the standard deviation of the particle size.

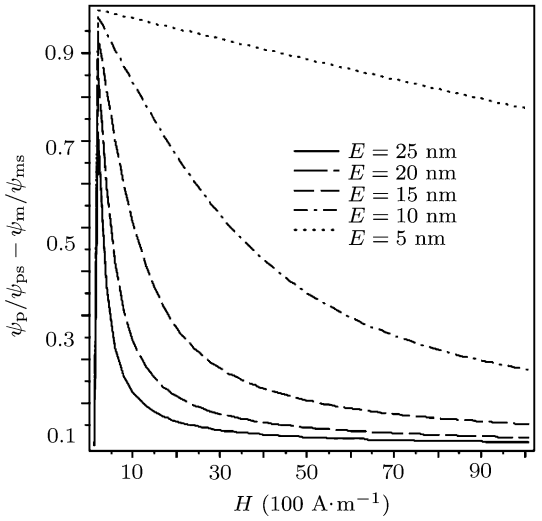


Fig. 5. The dependence curves of ($M_\mathrm{p}/M_\mathrm{ps}$–$M_\mathrm{m}/M_\mathrm{ms}$) versus H, for different mean particle sizes $E = 25$, 20, 15, 10, and 5 nm. For each of the mean size, the curves for $Sd = 10$, 7, 5 and 4 nm almost exactly overlap, thus the curves also represent the dependence of ($M_\mathrm{p}/M_\mathrm{ps}$–$M_\mathrm{m}/M_\mathrm{ms}$) versus H for $Sd = 10$, 7, 5 and 4 nm, with the different mean sizes $E = 25$, 20, 15, 10, and 5 nm.

4. Conclusions

Based on a lognormal model of particle size distribution, the polydispersity effects on the magnetization of a diluted ferrofluid are analysed. The results indicate that in comparison with the corresponding monodispersion, the lognormal polydispersity of the ferromagnetic nanoparticles leads to an increase of the saturation magnetization of the ferrofluid. Meanwhile, the effects also lead to a higher magnetization and a faster speed to magnetic saturation of the ferrofluid in an equivalent magnetic field.

For the effects on saturation magnetization, the latter is positively dependent on the standard deviation and negatively dependent on the mean value of the particle size. For a constant mean size, the saturation magnetization of the ferrofluids is positively dependent on the standard deviation; whereas for a constant standard deviation, the saturation magnetization presents a V-shape curve on the mean particle size, i.e., when the mean size is larger than the standard deviation, the saturation magnetization is positively dependent on the mean particle size, otherwise the saturation magnetization is negatively dependent

on the mean particle size. As for the polydispersity effects on the magnetization process of diluted ferrofluids, in an equivalent increasing magnetic field, the polydispersed ferrofluids have a higher magnetization value and a faster approach to saturation magnetization than the corresponding monodispersion. In a weak field, the normalized magnetizations of the polydispersed ferrofluid and the corresponding monodispersion have the maximum difference, whose value is positively dependent on the standard deviation and negatively dependent on the mean value of the particle size in the polydispersed ferrofluid.

For the example of magnetite ferrofluids, with the typical material parameters and a common dispersity $\sigma = 0.2$, calculations show that the lognormal polydispersity leads to a slight increase of the saturation magnetization but a noticeable increase of the speed to reach the saturation magnetization. The latter is noticeably dependent on the mean value, but little influenced by the standard deviation of the particle size. In summary, the common diluted ferrofluids of a lognormal polydispersity may be considered as monodisperse, as far as the size-dependent magnetization properties are concerned.

References

[1] Rosensweig R E 1998 *Ferrohydrodynamics* (Cambridge: Cambridge University Press) p. 7

[2] Thiesen B and Jordan A 2008 *Int. J. Hyperthermia* **24** 467

[3] Laurent S, Bridot J L, Elst L V and Muller R N 2010 *Future Med. Chem.* **2** 427

[4] Kaiser R and Miskolczy G 1970 *J. Appl. Phys.* **41** 1064

[5] Morozov K I and Lebedev A V 1990 *J. Magn. Magn. Mater.* **85** 51

[6] Bean C P and Livingston J D 1959 *J. Appl. Phys.* **30** 120S

[7] Shliomis M I 1974 *Usp. Fiz. Nauk.* **112** 427

[8] Coffey W T, Kalmykov Yu P and Waldron J T 2004 *The Langevin Equation* (Singapore: World Scientific) p. 11

[9] Morais P C, Garg V K, Oliveira A C, Silva L P, Azevedo R B, Silva A M L and Lima E C D 2001 *J. Magn. Magn. Mater.* **225** 37

[10] Morais P C, Santos R L, Pimenta A C M, Azevedo R B and Lima E C D 2006 *Thin Solid Films* **515** 266

[11] Leschhorn A, Embs J P and Lücke M 2006 *J. Phys.: Condens. Matter* **18** S2633

[12] Berkov D V, Görnert P, Buske N, Gansau C, Mueller J, Giersig M, Neumann W and Su D 2000 *J. Phys.* D: *Appl. Phys.* **33** 331

[13] Teixeira C B, Olavo L S F, Skeff Neto K and Morais P C 2007 *Hyperfine Interact.* **175** 113

[14] Brown W F 1963 *Phys. Rev.* **130** 1677

[15] Néel L 1949 *Ann. Geophys.* **5** 99

[16] Raikher Y L and Shliomis M I 1994 *Adv. Chem. Phys.* **87** 595

[17] Leslie-Pelecky D L and Rieke R D 1996 *Chem. Mater.* **8** 1770